RSC Advances


This is an *Accepted Manuscript*, which has been through the Royal Society of Chemistry peer review process and has been accepted for publication.

*Accepted Manuscripts* are published online shortly after acceptance, before technical editing, formatting and proof reading. Using this free service, authors can make their results available to the community, in citable form, before we publish the edited article. This *Accepted Manuscript* will be replaced by the edited, formatted and paginated article as soon as this is available.

You can find more information about *Accepted Manuscripts* in the Information for Authors.

Please note that technical editing may introduce minor changes to the text and/or graphics, which may alter content. The journal's standard Terms & Conditions and the Ethical guidelines still apply. In no event shall the Royal Society of Chemistry be held responsible for any errors or omissions in this *Accepted Manuscript* or any consequences arising from the use of any information it contains.

ROYAL SOCIETY OF CHEMISTRY

www.rsc.org/advances

Please do not adjust margins

RSC Advances

ARTICLE

# Synthesis and characterization of chiral PEDOTs enantiomers bearing chiral moieties in side chains: chiral recognition and its mechanism using electrochemical sensing technology

Received 00th January 20xx,
Accepted 00th January 20xx

DOI: 10.1039/x0xx00000x

www.rsc.org/

Liqi Dong, Long Zhang, Xuemin Duan*, Daize Mo, Jingkun Xu*, Xiaofei Zhu

In this work, we presented a pair of chiral PEDOT derivatives named by poly((*R*)-2-(chloromethyl)-2,3-dihydrothieno[3,4-b][1,4]dioxine) ((*R*)-PEDTC) and poly((*S*)-2-(chloromethyl)-2,3-dihydrothieno[3,4-b][1,4]dioxine) ((*S*)-PEDTC), which were empolyed as excellent chiral recognition materials for fabricating chiral sensors and then discriminating 3,4-dihydroxyphenylalanine (DOPA) enantiomers. Importantly, the mechanism of the stereospecificity of the interaction between DOPA enantiomers and chiral polymers was discussed specifically. A series of performance of corresponding polymers were characterized in some detail by different strategies including CV, CD, FT-IR, UV-Vis, SEM, and TG. CD spectrum indicated that (*R*)-PEDTC and (*S*)-PEDTC are mirror symmetric. CV presents that the polymers had superior redox reversibility in $CH_3CN$–$Bu_4NPF_6$. Finally, different electrochemical methods including CV, square wave voltammetry (SWV) and differential pulse voltammetry (DPV) were introduced for the discrimination of DOPA enantiomer. Satisfactory measurement results demonstrated that (*R*)-PEDTC/GCE and (*S*)-PEDTC/GCE exhibited excellent enantioselectivity to DOPA enantiomers and the tendency was the anisotropic interaction between (*R*)-PEDTC and *L*-DOPA, (*S*)-PEDTC and *D*-DOPA, respectively. That implied the obtained polymer films could be promising candidates as enantioselective materials in the electrochemical sensor field.

## 1. Introduction

Chiral conducting polymers refer to a class of conducting polymers (CPs) that possess chirality present some unique opportunities when used as chiral substrates or as chiral electrode materials.[1] They could, for example, find application in electrochemical chiral sensing or electrochemical asymmetric synthesis. Its research was began since 1985 *via* the electropolymerization of pyrrole monomers bearing chiral substituents ($R^*$) covalently attached to the pyrrole N centres by R. H. Baughman *et al.*[2] Soon afterwards, Chiral polythiophenes was synthesized by M. Lemaire *et al.* under an asymmetric reaction field consisting of chiral nematic ($N^*$) liquid crystals.[3] From then on, a great number of studies on chiral conducting polymers including polypyrrole (Ppy)[4] polyanilines (PANI),[5-7] polyacetylene,[8] polyfluorenes (PFs),[9, 10] polythiophenes (PTs),[11-14] and thienylene–phenylene copolymers[15-17] have emerged rapidly. It is amazing that chiral CPs have been made tremendous advancement in such short history for developing various applications using their particular properties, such as chiral discrimination,[18-20] chromatographic separation,[21, 22] asymmetric catalysis,[23-25] optoelectronic devices and batteries,[26] photoisomerization switching[27] and controlled release drug delivery.[28, 29]

Among the chiral CPs, chiral poly(3,4-ethylenedioxythiophene) (PEDOT) emerging as a "superstar" material has attracted tremendous attention due to its unique structure and electronic property.[30, 31] Comparing with racemic PEDOT, introduction of a chiral moiety into a side chain could reduce the rigidity of polymer chains and have a positive impact on solubility, thermal stability, and orientation as liquid crystal materials.[1, 32, 33] Despite the fact that chiral PEDOTs have been synthesized in 2004 by K. Akagi et al.,[31] immense challenges have been encountered for their applications, and only a few studies have been dedicated to form nematic liquid crystal.[34, 35] However, some hot applications, such as molecular recognition, enantioselective separation, microstructure control and asymmetric catalysis are still lack of basic exploration. Therefore, exploring the potential application of chiral PEDOT will provide the inspiration on the further design of novel chiral PEDOT derivatives, which would lead to innovative changes in the development of chiral PEDOTs.

Some recent study in our group showed that chiral PEDOTs bearing chiral moieties in side chains might be candidates to enable recognized enantiomers.[36, 37] Reasonable use allows us to study and to control the behavior of the polymers which make them very valuable in chiral recognition. On one hand, to the best of our knowledge, the chiroptical activity property of PEDOTs owing to incorporation chirality has already been reported.[36] But the field of

*School of Pharmacy, Jiangxi Science & Technology Normal University, Nanchang, 330013, China.*
*Fax: +86-791-83823320, Tel.: +86-791-88537967*
*E-mail: duanxuemin@126.com (X. Duan), xujingkun@tsinghua.org.cn (J. Xu)*
Electronic Supplementary Information (ESI) available: [$^1$H NMR spectrum of (*R*)-and (*S*)-EDTC, table of assignment for FT-IR Spectra, table of thermogravimetric Parameters for (*R*)- and (*S*)-PEDTC.]. See DOI: 10.1039/x0xx00000x

RSC Advances Accepted Manuscript



Please do not adjust margins

using this property for the enantiomers recognition is still preliminary. The homochiral selective electrode for discriminate enantiomers and its mechanism still remains unexplored even the gap between enantiomers also have chance to get further lager. Hence, understanding the mechanism of chiral recognition, and then pursuing the larger gap between two enantiomers and more efficient chiral electrode materials to develop the application of chiral PEDOTs is valuable and fascinating. On the other hand, to date, the dominant approaches for chiral recognition are chromatographic methods (including high performance liquid chromatography (HPLC),[38-40] gas chromatography (GC),[41-43] chiral ligand exchange chromatography (CLEC),[44] supercritical fluid chromatmography (SFC)[45, 46]), spectroscopic characterizations (including fluorescence detection (FL),[47, 48] vibrational circular dichroism (VCD)[49]), capillary electrophoresis (CE) [50, 51] and molecular imprinting polymer techniques (MIP).[52, 53] Even if these techniques are fairly efficient, they are usually time consuming, equipments costly and need sophisticated and extensive analysis procedures. However, electrochemical strategies offer some advantages over the other techniques such as low cost, simple equipment, on-line measurement and high sensitivity.[54-58] Thus, the combination of electrochemical molecular recognition approach and chiral PEDOT materials can be potentially utilized to fabricate a chiral electrochemical sensor.

In this article, we synthesized a pair of PEDOT enantiomers *i. e.* (*R*)-PEDTC and (*S*)-PEDTC and systematically investigated the electropolymerization behavior, electrochemical properties, structural characterization, circular dichroism, morphology and thermal stability. Finally, (*R*)-/(*S*)-PEDTC as chiral materials modified glassy carbon electrodes (GCEs) were successfully employed to recognize 3,4-dihydroxyphenylalanine(DOPA) enantiomers. Satisfactory results implied that the obtained polymer films could be a promising candidate in the chiral recognition field.

## 2. Experimental section

### 2.1 Chemicals and Materials

All materials were reagent grade and were used directly without further purification unless otherwise noted. 3,4-Dimethoxythiophene (98%, AR) was purchased from Vita Chemical Reagent Co. Ltd (Shanghai China). (*R*)-3-choro-1,2-propanediol (99%, 98% e.e.) and (*S*)-3-choro-1,2-propanediol (99%, 98% e.e.) were purchased from Daicel Chiral Technologies Co., Ltd (Shanghai China). *p*-Toluenesulfonic acid monohydrate (*p*-TSA, 99%, AR), *L*-/*D*-3,4-dihydroxyphenylalanine (*L*-/*D*-DOPA, 99%, GR), ammonia solution ($NH_3 \cdot H_2O$, 25-28%, AR), Potassium bromide (KBr, 99%, IR) and sulfuric acid ($H_2SO_4$, 98%, AR) were purchased from Aladdin Industrial Inc (Shanghai China). Acetonitrile ($CH_3CN$, AR) was purchased from Sinopharm Chemical Reagent Co. Ltd. Dimethyl sulfoxide (DMSO, 99%, AR) was purchased from Lingfeng Chemical Reagent Co. Ltd. Toluene (AR; Xilong Chemical Co., Ltd.) was purified by sulfuric acid and dried with anhydrous calcium chloride. Indium tin oxide (ITO) coated glass was purchased from Zhuhai Kaivo Optoelectronic Technology Co., Ltd. Tetrabutylammonium hexafluorphosphate ($Bu_4NPF_6$, 99%, Energy Chemical Reagent Co., Ltd.) was dried under vacuum at 60 °C for 24 h before use. Double-distilled deionized water used directly without further purification.

### 2.2 Electrosynthesis and Electrochemical Tests

Electrochemical polymerization was carried out using 0.01 M (*R*)-/(*S*)-2-(chloromethyl)-2,3-dihydrothieno[3,4-b][1,4]dioxine ((*R*)-/(*S*)-EDTC) in $CH_3CN$-$Bu_4NPF_6$ (0.1 M) systems. Prior to polymerization, all the solutions were deaerated by a dry nitrogen stream for 15 min and maintained under a slight overpressure during the electrochemical experiments to avoid the effects of oxygen. Film thickness was controlled by the total charge passed through the cell, which was read directly from the current-time (I-t) curves by computer. After polymerization, the polymer films were washed repeatedly with acetonitrile to remove the electrolyte and monomer/oligomers.

All of the electrochemical tests were conducted in monomer-free solvent-electrolytes in a one-compartment cell with the use of CHI 660D electrochemistry workstation (Shanghai Chenhua Instruments Co., China) under computer control. Two Pt wires with diameter of 1 mm were used as the working electrode and counter electrode, respectively. An Ag/AgCl electrode dipped in the solution served as the reference electrode, and it revealed sufficient stability during the experiments. Electrodes mentioned above were carefully polished with abrasive paper (1500 mesh), and cleaned by deionized water and acetone successively before each examination.

### 2.3 Apparatus of Chiral Sensor

Cyclic voltammetry (CV), square wave voltammetry (SWV) and differential pulse voltammetry (DPV) measurements were achieved with a CHI 660D electrochemistry workstation. A conventional three-electrode system was employed, including a bare or modified glass carbon electrode (GCE) as working electrode, a platinum wire and a saturated calomel electrode (SCE) as counter electrode and reference electrode, respectively. (*R*)-PEDTC/GCE and (*S*)-PEDTC/GCE were obtained individually by one-step electropolymerisation of 10 mM monomers on GCE at a constant potential of 1.1 V *vs.* SCE in $CH_3CN$-$Bu_4NPF_6$ system and the deposition time was 40 s. Then, the films were washed repeatedly with double-distilled deionized water to remove the electrolyte monomers and dried in air. All measurements were conducted at room temperature (25±2 °C).

### 2.4 Characterization

$^1H$ NMR spectra were recorded on a Bruker AV 400 NMR spectrometer with chloroform-*d* as the solvent and tetramethylsilane (TMS) as an internal standard. Infrared spectra (FT-IR) were recorded using Bruker Vertex 70 Fourier spectrometer with samples in KBr pellets. The resolution ratio is 2 $cm^{-1}$. Scanning electron microscopy (SEM) measurements were taken using a JSM-6701F cold field emission scanning electron microscope with the polymer deposited on the ITO-coated glass. Circular dichroism (CD) spectroscopy (JASCO J-720) was used to characterize the polymer films. Fluorescence spectra of the monomer and polymer were determined with an F-4500 fluorescence spectrophotometer (Hitachi). Thermogravimetric analysis (TGA) was performed with a Pyris Diamond TG/DTA thermal analyzer (Perkin-Elmer) under a nitrogen stream from 25 to 1100°C at a heating rate of 10 °C/min.

RSC Advances Accepted Manuscript



This journal is © The Royal Society of Chemistry 20xx

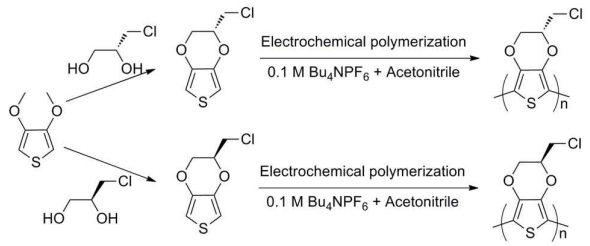


**Scheme 1** The synthesis route of (*R*)-/(*S*)-EDTC enantiomers and its electropolymerization.

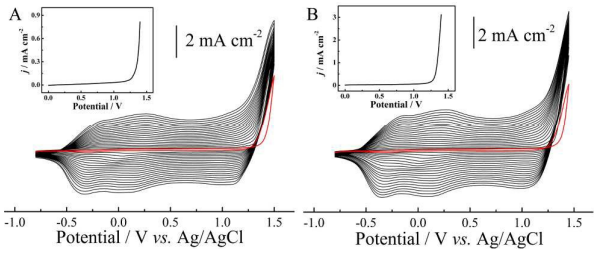


**Figure 1** Cyclic voltammograms (CVs) of (*R*)-EDTC (A) and (*S*)-EDTC (B) electropolymerized in $CH_3CN$ containing 0.1 M $Bu_4NPF_6$ and 0.01 M monomers at potential scan rate of 50 mV $s^{-1}$. Inset: corresponding anodic polarization curve of (*R*)-/(*S*)-EDOTC enantiomers.

To obtain a sufficient amount of polymer for characterization, Pt and stainless-steel sheets with a surface area of 4 and 6 $cm^2$ each were employed as the working and counter electrodes, respectively. An Ag/AgCl electrodes directly immersed in the solutions served as the reference electrode. For spectral analyses, the polymer films were de-doped with 25% hydrazine hydrate for 3 days and then washed repeatedly with pure water. Finally, the polymer film was dried at 60 $^oC$ under vacuum for 24 h.

### 2.5 Syntheses of (*R*)-/(*S*)-EDTC

To a well-stirred solution of 3,4-dimethoxythiophene (16.300 g, 113.05 mmol) in 280 mL of dry toluene, (*R*)-3-choro-1,2-propanediol or (*S*)-3-choro-1,2-propanediol (25.620 g, 231.77 mmol), and *p*-toluenesulfonic acid monohydrate (1.600 g, 9.29 mmol) were added under a nitrogen atmosphere. The solution was heated at 90$^o$C for 72 h. Then, another of (*R*)- or (*S*)- diol (25.620 g, 231.77 mmol) was added, and the solution was heated at 90 $^o$C for another 3 h and was allowed to cool to room temperature. After removal of the solvent, the remaining crude product was isolated by column chromatography (silica gel, petroleum ether/acetic ether, 10/1, v/v) to give 12.525 g of a white solid (yield 58%) for (*R*)-EDTC or to give 10.666 g of a white solid (yield 49%) for (*S*)-EDTC.

(*R*)-EDTC: $[\alpha]_D^{25}$ = -2.300 (c = 1 g /100mL, in $CHCl_3$) $^1$H NMR (400 MHz, $CDCl_3$, ppm) $\delta$: 6.27 (d, $J$ = 4 Hz, 2H), 4.30-4.24 (m, 1H), 4.20-4.16 (m, 1H), 4.08-4.05 (m, 1H), 3.65-3.54 (m, 2H). $^1$H NMR spectrum was showed in Supporting Information Figure S1.

(*S*)-EDTC: $[\alpha]_D^{25}$ = +2.300 (c = 1 g /100mL, in $CHCl_3$) $^1$H NMR (400 MHz, $CDCl_3$, ppm) $\delta$: 6.27 (d, $J$ = 4 Hz, 2H), 4.30-4.24 (m, 1H), 4.20-4.16 (m, 1H), 4.08-4.03 (m, 1H), 3.65-3.54 (m, 2H). $^1$H NMR spectrum was showed in Supporting Information Figure S2.

## 3. Results and Discussion

### 3.1 Syntheses of Monomers

The racemic mixtures 2-chloromethyl-2,3-dihydrothieno[3,4-b][1,4]dioxine (EDTC) have been reported.[59-61] Based on the works of scientists previously, the EDTC was developed by reacting 3,4-dimethoxythiophene and 3-chloro-1,2-propanediol enantiomers in an acid-catalyzed trans-etherification reaction (Scheme 1). The chirality of EDTC was introduced by bring in a chiral source *i.e.* (*R*)-/(*S*)-3-choro-1,2-propanediol. Noteworthy, the 3-choro-1,2-propanediol enantiomers as chiral source have already confirmed, which means the chirality of (*R*)- or (*S*)-EDTC will not be changed in synthetic process. Thus, two single chiral EDTC monomers were obtained.

### 3.2 Electrochemical Polymerization

The successive CVs of (*R*)-EDTC (A) and (*S*)-EDTC (B) in $CH_3CN$-$Bu_4NPF_6$ systems at a potential scanning rate of 50 mV $s^{-1}$ are illustrated in Figure 1. In the first cycle of CVs, the current densities on the reverse scan were higher than those on the forward scan (in the region of -0.8-1.5 V for (*R*)-EDTC and -0.8-1.45 V for (*S*)-EDTC, respectively). The formation of this loop could be explained as the characteristics of nucleation process.[62] The redox peaks of (*R*)-EDTC and (*S*)-EDTC appeared near +0.25 V and +0.14 V, -0.16 V and -0.33 V. These peaks were assigned to the *p*-doping/dedoping processes of (*R*)-EDOTC and (*S*)-EDTC film formed in previous scans. Upon subsequent potential scanning, progressive increase of peak currents densities and decrease of oxidation onset potentials could be seen in subsequent scans, indicating the gradually growing amount of the polymer film with increased number of monomeric units deposited onto the electrode surface (light-blue to blue-back as the deposit thickened).[63] In fact, the formation of a compact and homogeneous film on the electrode surface was observed. Apparently, both the electrochemical polymerization of (*R*)-EDTC and (*S*)-EDTC and the onset oxidation potential ($E_{ox}$) of (*R*)-EDTC (1.26 V, Figure 1A inset) and (*S*)-EDTC (1.27 V, Figure 1B inset) were extraordinarily analogous. In addition, the $E_{ox}$ of other EDOT and analogues such as EDOT, EDTM and C4-EDOT-COOH were 0.92 V, 0.88 V, and 0.99 V,[64, 65] which were lower than (*R*)-/(*S*)-EDTC. The results indicated that the oxidation of (*R*)-/(*S*)-EDTC were harder than EDOT and its analogues.

### 3.3 Structural Characterization

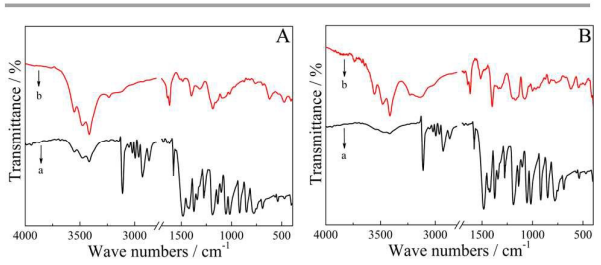


**Figure 2** FT-IR spectra of (*R*)-PEDTC (A) and (*S*)-PEDTC (B): monomers (a) and polymers (b).

RSC Advances Accepted Manuscript

FT-IR spectra of the monomers and their corresponding polymers were recorded to elucidate their structure and interpret the polymerization mechanism. The detail peak assignment and comparison for (*R*)-EDTC, (*R*)-PEDTC, (*S*)-EDTC and (*S*)-PEDTC were summarized in Supporting Information Table S1. The results were similar to previous report of racemic mixture EDTC.[60] In the functional group region, the peak at 3111 $cm^{-1}$ in the monomers spectrum of (*R*)-EDTC and (*S*)-EDTC is attributed to the =C−H stretching vibration which disappeared/weakened in the spectrum of (*R*)-PEDTC and (*S*)-PEDTC. This phenomenon is a direct proof that the electrochemical polymerization of (*R*)-EDTC and (*S*)-EDTC occurring at $\alpha$-positions of thiophene ring. In the fingerprint region, the emergence characteristic peaks located at 1021$cm^{-1}$ and 919 $cm^{-1}$ for (*R*)-EDTC, 1016 $cm^{-1}$ and 920 $cm^{-1}$ for (*S*)-EDTC should assigned to in-plane deformation vibration and out-of-plane deformation vibration. However, all these peaks disappeared in FT-IR spectrum of the polymers, which further confirmed that (*R*)-PEDTC and (*S*)-PEDTC were dominantly electropolymerized through $\alpha,\alpha'$-coupling of EDOT units. Typically, for all the monomers and polymers the peaks at approximately 1186-1102 $cm^{-1}$ and 836-875 $cm^{-1}$ could be attributed to asymmertic and symmetric C-O stretching vibration, respectively. Further, the vibration nearly 1482 $cm^{-1}$ is ascribed to the stretching mode of C=C bond, while the peaks at 1375, 1275, 1055 $cm^{-1}$ results from the stretching of single C−C bond and the =C-O-C vibration, respectively. For the chlorine atom, the absorption peaks originated from the C-Cl stretching and deformation vibrations could be observed at 770 and 543 $cm^{-1}$, respectively.

In addition, both the (*R*)- and (*S*)-PEDTC exhibit essentially identical (as expected) characteristic absorption bands, with peaks similar to those of racemic PEDTC prepared by electrochemical polymerization, indicating that the two films consist of repeating units of EDTC. Besides, the absorption bands in the spectra of the doped polymers were obviously broadened in comparison with those monomers, similar to those of other conducting polymers.[63, 64, 66] This phenomenon was probably due to the fact that the resulting product was composed of oligomers/polymers with wide chain dispersity.

### 3.4 Optical Properties

The as-prepared PEDTC films in the doped state were dark blue in color. When the films were dedoped by 25% ammonia for 3 days, their colour changed to brownish yellow. However, the resulting PEDTC films were found to be incompletely soluble in DMSO or THF, also exhibited poor solubility in other solvents such as acetonitrile and acetone.

UV–*Vis* spectra of the monomers and polymers dissolved in DMSO were examined in Figure 3. The monomers of (*R*)-EDTC and (*S*)-EDTC showed a characteristic absorption peak at about 265 and 271 nm, respectively (Figure 3 inset). For (*R*)-PEDTC and (*S*)-PEDTC, the trend of absorbance curves and the position of peaks were similar to PEDOT.[67] In the neutral state of polymers, the peak at about 590 nm was attributed to $\pi$-$\pi^*$ transition. Meanwhile, in the oxidized state, the polymer films showed not only the absorption at 590 nm but also a broad peak at wavelengths longer than 940 nm. This wide peak is associated with the bipolaron band in the spectrum. This result confirmed the occurrence of electrochemical polymerization among the monomers and the formation of a conjugated polymer with broad molar mass distribution. Also, the absorption band at 590 nm in the neutral state and the broad band located from 900 to 1000 nm in the oxidized state are responsible for the light-blue and black-blue colours in the dedoped and doped films, respectively. In other words, the reversible electrochromic change occurs through the electrochemical doping and dedoping. In addition, it should be noted that the spectrum of doped and dedpoed polymer was consistency, which mainly because the automatic dedoping process of the polymer.[68]

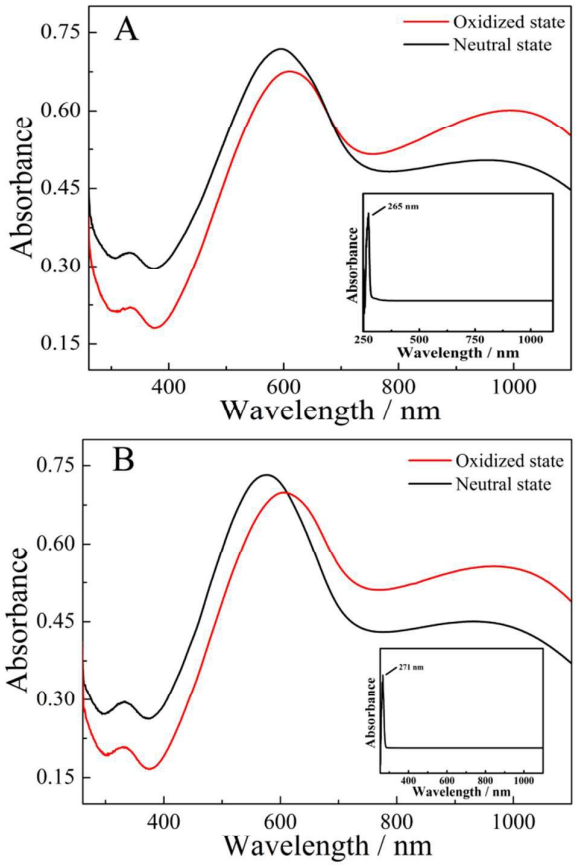


**Figure 3** UV-*Vis* spectra of (*R*)-PEDTC (A) and (*S*)-PEDTC (B) in neutral and oxidized states. Solvent: DMSO.

Circular dichroism (CD) spectra of the polymers are shown in Figure 4. As shown in Figure 4, (*R*)- and (*S*)-PEDTC exhibit a strong Cotton effect in the neutral state, but no Cotton effect was observed in the oxidized state. In neutral state, at wavelength about 300 nm (*R*)-PEDTC exhibits negative Cotton effect while (*S*)-PEDTC displays positive effect in CD measurements. That is to say, the CD spectra of (*R*)-PEDTC and (*S*)-PEDTC are mirror symmetric but otherwise essentially identical. In the oxidized state, the CD spectra of the polymers showed a decrease in intensity and an inversion in the sign of the Cotton effect. It is suggested that the changes of CD bands in the neutral and oxidized states might be related to a chirality change in the polymers. Therefore, the CD band could be

RSC Advances Accepted Manuscript



This journal is © The Royal Society of Chemistry 20xx

Please do not adjust margins

Please do not adjust margins



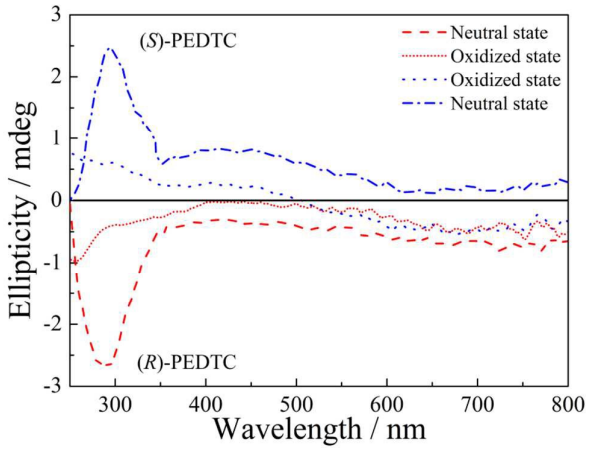


**Figure 4** CD spectra of neutral and oxidized (*R*)-PEDTC and (*S*)-PEDTC. Solvent: DMSO.

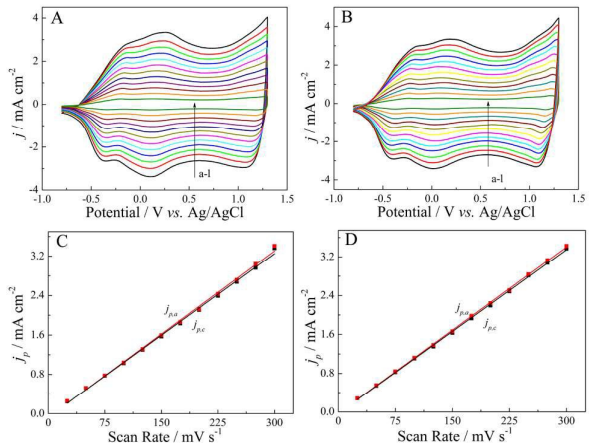


**Figure 5** CVs of (*R*)-PEDTC (A) and (*S*)-PEDTC (B)-coated Pt electrode in monomer-free $CH_3CN$-$Bu_4NPF_6$ (0.1 M) systems at potential scan rates from 300 to 25 mV $s^{-1}$ with potential decrement of 25 mV $s^{-1}$. (C, D) Plots of anodic ($j_{p,a}$) and cathodic ($j_{p,c}$) peak currents densities *vs.* potential scan rates, respectively.

observed in the neutral polymers were ascribed to two factors: (i) The neutral polymers have a relatively high degree of freedom in terms of internal rotation of the main chain. (ii) Conversely, when the polymer was oxidized through doping, the planarity of the main chain is enhanced due to the dopants ($PF_6^{-1}$) were intercalated into the main chain.[11, 31, 69]

Besides, as can be seen in Figure 4, the intensity of CD spectra was weaker than other chiral polymers with similar structures reported previously.[8, 14, 31] That mainly attributed to the small chiral group (Cl atom) and regioirregular polymers. Theoretically, the regioregularity of polymer could form head-to-head (HH) or head-to-tail (HT), and it is assumed that such structural changes affect the optical properties of the polymer. However, control of the regioregularity of the polymer is difficult to achieve by this electrochemical polymerization method, which tends to form polymers with random HH and HT regularities.[17]

### 3.5 Electrochemistry Properties

For a comparative study, the electrochemical behaviors of both (*R*)-PEDTC and (*S*)-PEDTC films were carried out in monomer-free $CH_3CN$–$Bu_4NPF_6$, as shown in Figure 5. Similar to other EDOT-based polymers, both (*R*)-PEDTC and (*S*)-PEDTC films exhibited broad anodic and cathodic peaks in the $CH_3CN$-$Bu_4NPF_6$ system.[62-64, 68] Also, the electrochemical performance of (*R*)-PEDTC and (*S*)-PEDTC were extremely similar to each other. All peak current densities were well proportional to the potential scanning rate (Figure 5 C and D), which indicated that the redox process was non-diffusional and electroactive materials were anchored to the surface of working electrode. Furthermore, the calculated $j_{p,a}/j_{p,c}$ values ($j_{p,a}$ or $j_{p,c}$ is calculated as the ratio between anodic or cathodic peak current density and potential scan rate) of (*R*)-PEDTC and (*S*)-PEDTC are both very closer to 1.0, demonstrating the polymers had superior redox reversibility in $CH_3CN$–$Bu_4NPF_6$. It was also found that the discrepancy in the redox peak potentials of (*R*)-PEDTC and (*S*)-PEDTC were obvious. The main reasons that account for this phenomenon are usually as follows: slow heterogeneous electron transfer, local rearrangement of polymer chains, slow mutual transformation of various electronic species, and electronic charging of interfacial exchange corresponding to the metal/polymer and polymer/solution interfaces.[70] It is worth noting that (*R*)-PEDTC and (*S*)-PEDTC display very similar electrochemical behavior, probably because the chirality of the polymers does not affect the redox behavior.[17]

As we all know, the good stability of conducting polymers is a key property for their application in advanced technological applications.[71] Therefore, the long-term stability of these polymers was investigated in a monomer-free electrolyte solution by applying potential pulses at a potential scan rate of 150 mV $s^{-1}$, as shown in

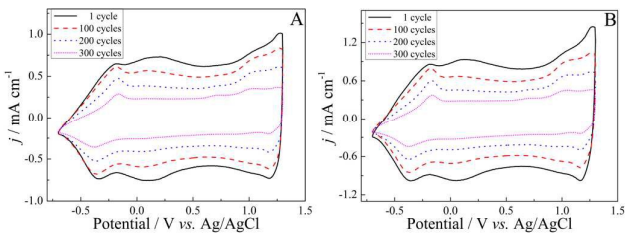


**Figure 6** Long-term CVs of (*R*)-PEDTC (A) and (*S*)-PEDTC (B) in monomer-free $CH_3CN$–$Bu_4NPF_6$ (0.1 M) upon repeated cycling at a scan rate of 150 mV $s^{-1}$.

RSC Advances Accepted Manuscript



Please do not adjust margins

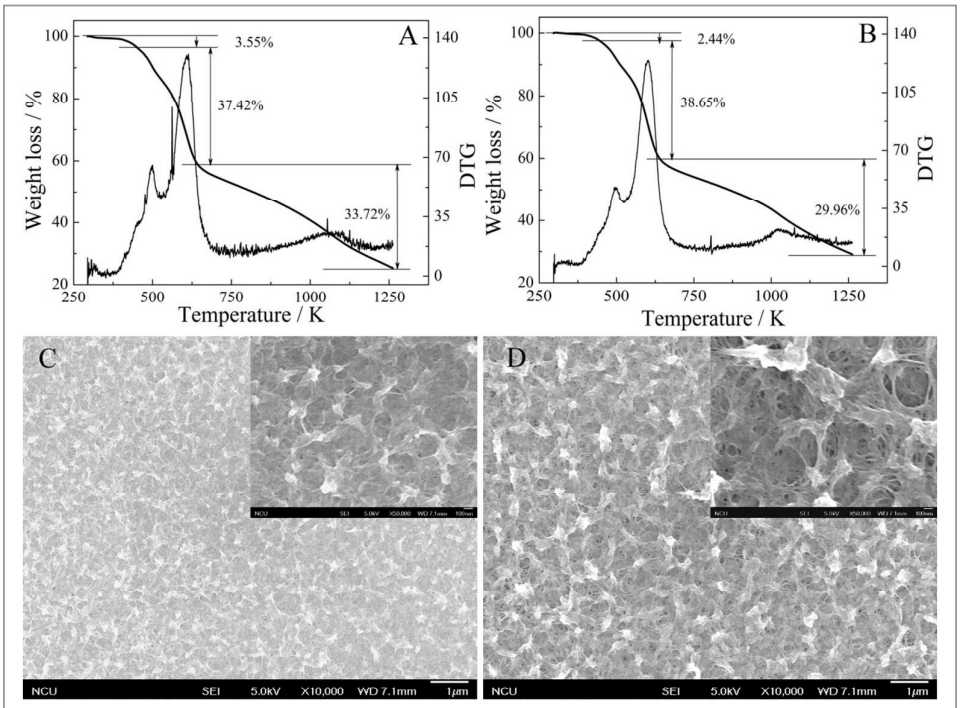


**Figure 7** A, B: TG and DTG curves of (*R*)-PEDTC (A) and (*S*)-PEDTC (B) under a nitrogen atmosphere. C, D: SEM micrographs of (*R*)-PEDTC (C) and (*S*)-PEDTC (D) films deposited electrochemically on the ITO/glass electrode in $CH_3CN$-$Bu_4NPF_6$ (0.1 M) systems containing 0.01 M monomers. Deposition time: 30 s; ITO/glass dimension: 0.5 × 0.5 × 0.1 $cm^3$ (magnification: 10,000 ×, inset: 50,000 ×).

Figure 6. On the basis of exchange charge, the electrochemical activities of (*R*)-PEDTC and (*S*)-PEDTC were preserved up to 84% and 78% after 100 cycles, respectively. Whereas, the electrochemical activities of these polymers maintained only about 37% of the exchange charge retained after 300 cycles. Overall, both (*R*)-PEDTC and (*S*)-PEDTC experienced an apparent degradation just after 100 cycles. (*R*)-PEDTC displayed better stability, comparable to (*S*)-PEDTC. All the results demonstrate a relatively high electrochemical stability of (*R*)-PEDTC and (*S*)-PEDTC, which providing an excellent basis for using the polymers in chiral recognition experiments.[54, 56, 57, 64]

### 3.6 Thermal Properties and Surface Morphology

Thermogravimetric analytical experiments were performed under a nitrogen stream in the temperature range of 298-1260 K with a heating rate of 10 K $min^{-1}$. According to Figure 7A and B, it can be clearly observed that there were typically three-step weight losses for both (*R*)-PEDTC and (*S*)-PEDTC: (i) 3.55% weight loss of the polymer occurred before 448 K, (ii) a rapid weight loss was in the range of temperature 449-654 K, (iii) the total weight loss at 1260 K was calculated to be 75% based on the initial weight. These above results are comparable to the reported residue of PEDOT (20%).[72] Compared with parent PEDOT prepared in aqueous micellar solution[73] or $CH_2Cl_2$-$Bu_4NBF_4$[72], (*R*)-PEDTC and (*S*)-PEDTC films showed reasonably good thermal stability. The detailed thermogravimetric parameters of (*R*)-/(*S*)-PEDTC were summarized in Supporting Information Table S2.

For analyzing the surface morphology, constituent, and texture of (*R*)-PEDTC and (*S*)-PEDTC, scanning electron microscopy (SEM) has been performed (Figure 7). Macroscopically, as-formed (*R*)- and (*S*)-PEDTC films was compact, helical and blue in color. Microscopically, the (*R*)-PEDTC film had a rather compact, porous network structure, meanwhile the (*S*)-PEDTC film displayed well-entangled and interconnected, loose and porous network morphology. The morphologies of (*R*)- and (*S*)-PEDTC films were parallel. However, at high magnifications (50 000×), the (*R*)-PEDTC film appeared to be a little swollen and more compact (inset of Figure 7C and D). In addition, these morphologies of polymer films were extremely beneficial to the immobilization of biologically active species due to the large surface area and high absorption ability of network morphology.[74]

### 3.7 Chiral Recognition

According to other publications,[54, 56, 75] 0.25 M $H_2SO_4$ was selected as electrolytes and usually employed to recognition of DOPA enantiomers. It can be clearly seen in Figure 8 A and B(dotted line), there was no redox electrochemical response at modified electrode in 0.25 M $H_2SO_4$, which could eliminate the impact of the electrolytes on the experiment. Whereas a pair of apparent redox peaks appeared around 0.55V when added *D*-DOPA and *L*-DOPA in 0.25 M $H_2SO_4$, ascribing to two-electron-two-proton oxidation and reduction of the dopa/dopaquinone couple.[76] That means both (*R*)-PEDTC/GCE and (*S*)-PEDTC/GCE had Faradic response for DOPA enantiomers and the redox peaks were corresponded to electrochemical behavior of

RSC Advances Accepted Manuscript


This journal is © The Royal Society of Chemistry 20xx

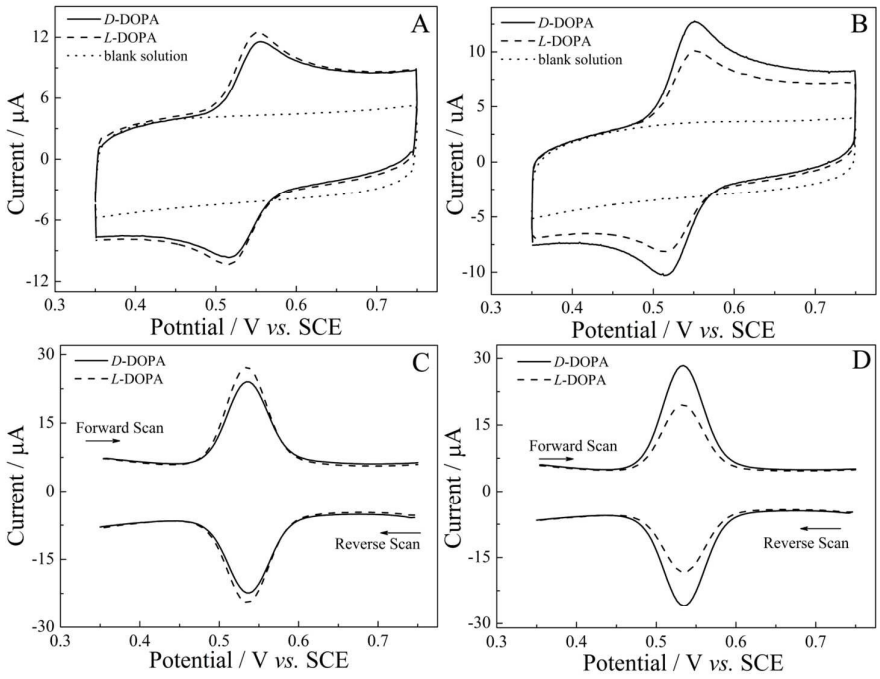


**Figure 8** CVs and SWVs of (*R*)-PEDTC (A and C) and (*S*)-PEDTC (B and D) modified electrodes in 0.25 M $H_2SO_4$ containing 0.25 mM *L*-DOPA (dashed line) or *D*-DOPA (solid line). CV: scan rate, 50 mV $s^{-1}$; SWV: step height, 0.004 V; frequency, 5 Hz.

DOPA.[76] As illustrated in Figure 8 A and B, similar CV curves and a little difference of peak currents for *D*-DOPA and *L*-DOPA were observed. For (*R*)-PEDTC/GCE, the anodic peak current value of *D*-DOPA or *L*-DOPA was 11.56 or 12.47 μA, and the cathodic was -9.76 or -10.42 μA. For (*S*)-PEDTC/GCE, the anodic peak current value of *D*-DOPA or *L*-DOPA was 12.74 or 10.13 μA, and the cathodic one was -10.34 or -8.17 μA. Though, DOPA enantiomers can be recognized by CV technology, the gap of peak currents was unremarkable. Thus, further analyses using SWV technology revealed striking evidence of chiral discrimination and larger electrochemical response signals were obtained for (*R*)-/(*S*)-PEDTC to the DOPA enantiomers (Figure 8(C, D)). For (*R*)-PEDTC, the anodic peak current value of *D*-DOPA or *L*-DOPA was 24.09 or 27.37 μA in the forward scan, and the cathodic peak current value was -22.40 or -24.51 μA in reverse scan. For (*S*)-PEDTC/GCE, the anodic peak current value of *D*-DOPA or *L*-DOPA was 28.31 or 19.16 μA (forward scan), and the cathodic one was -26.11 or -18.47 μA (reverse scan). These results clearly indicated that a clear chiral discrepancy was observed: (*R*)-PEDTC/GCE showed higher peak current response towards *L*-DOPA; while the contrary phenomenon occurred on (*S*)-PEDTC/GCE. That is to say the heterochiral interaction between (*R*)-/(*S*)-PEDTC and *L*-/*D*-DOPA was considerably more favorable than the homochiral interaction. Such differences in the current change make this sensor have practical application potential for the enantioselective recognition of the DOPA enantiomers.

Besides, in order to gain further evidences for (*R*)-PEDTC and

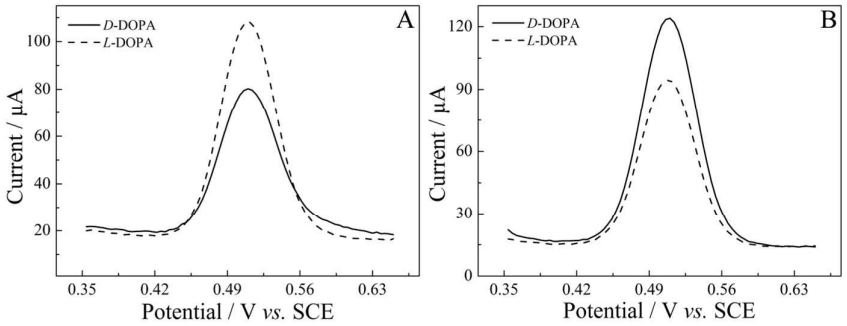


**Figure 9** DPVs of (*R*)-PEDTC (A) and (*S*)-PEDTC (B) modified electrodes in 0.25 M $H_2SO_4$ containing 0.25 mM *D*-DOPA (solid line) or *L*-DOPA (dashed line). DPV: increasing potential, 0.004 V; amplitude, 5 Hz; pulse width, 0.2 s; pulse period, 0.5 s.

RSC Advances Accepted Manuscript

(*S*)-PEDTC have enantioselectivity to DOPA enantiomers, DPV technology was chosen for further study. Also, distinctive difference in peak current values could be seen in Figure 9: the peak current value of *D*-DOPA or *L*-DOPA on (*R*)-PEDTC was 80.09 or 108.24 μA, while the peak current values of *D*-DOPA or *L*-DOPA on (*S*)-PEDTC was 124.16 or 94.22 μA. The experiment results of SWVs and DPVs were essentially identical, confirming that (*R*)-PEDTC/GCE and (*S*)-PEDTC/GCE exhibited excellent enantioselectivity to DOPA enantiomers and the tendency was the anisotropic interaction between (*R*)-PEDTC and *D*-DOPA, (*S*)-PEDTC, and *L*-DOPA.

## Discussion

The elucidation of chiral recognition mechanism is the key question for chiral recognition. Herein, we consider the mechanism of chiral recognition underlying DOPA enantiomers based on the present experimental results as shown in Chart 1. The electrochemical sensing process usually consists of two steps: analyte recognition and signal generation.[19]

At the stage of analyte recognition, the interaction between polymer modified electrode and DOPA enantiomers, and the redox reaction of DOPA are two parts of this step. Marzieh Eslami *et al.*[76]demonstrated that the amine and carboxyl groups of DOPA at low pHs will be protonated, and the molecules will be in acidic form. Therefore, the nucleophilic property of the amine group is removed through protonation. These efforts can be rationalized as a consequence by formation of hydrogen bonds that link to the polymer surface (Chart 1B).[77] Then, when DOPA enantiomers were attached to the surface of the modified electrode, the left-handed DOPA (*L*-DOPA) is easier to connected to the (*R*)-PEDTC/GCE (right-handed) while the right-handed DOPA (*D*-DOPA) is hindered.[78] Conversely, (*S*)-PEDTC has the opposite pattern against the *D*-DOPA and *L*-DOPA. Therefore, the selective response may be attributed to the fact that the conformation of *L*-DOPA is more inclined to interact with (*R*) form polymer than *D*-DOPA, whereas the D-DOPA is more delighted to interact with (*S*)-PEDOT than L-DOPA. In other words, the heterochiral interaction between polymer modified electrodes and DOPA enantiomers is considerably more favour than the homochiral interaction. Since most of the DOPA molecules in strong acidic pH (0.25 M $H_2SO_4$) are in acidic form, they have a repulsion force with each other, and the probability of the dimerization chemical reaction is insignificant. The mechanism of the hydrolysis chemical reaction is shown in Chart 1C.[54, 76]

During the signal generation of SWV and DPV, the staircase scan waveform could effectively extend the interaction time between electrode and DOPA. After many cycles, the enantioselectivity is finally amplified and thus the DOPA enantiomers are discriminated.[79] This is highly consistent with the fact that the chiral selectivity is attributed to the preferential interaction between chiral selector and one of the enantiomers.[54, 56, 75, 78]

## 4. Conclusions

In summary, a pair of chiral enantiomers of EDOT derivatives was synthesized. The corresponding polymers (*R*)-PEDTC and (*S*)-PEDTC were prepared for the first time by electrochemical polymerization, and the polymers showed good redox activity and stability in monomer-free electrolytes. The enantiomers of (*R*)-PEDTC and (*S*)-PEDTC were almost the same as each other in terms

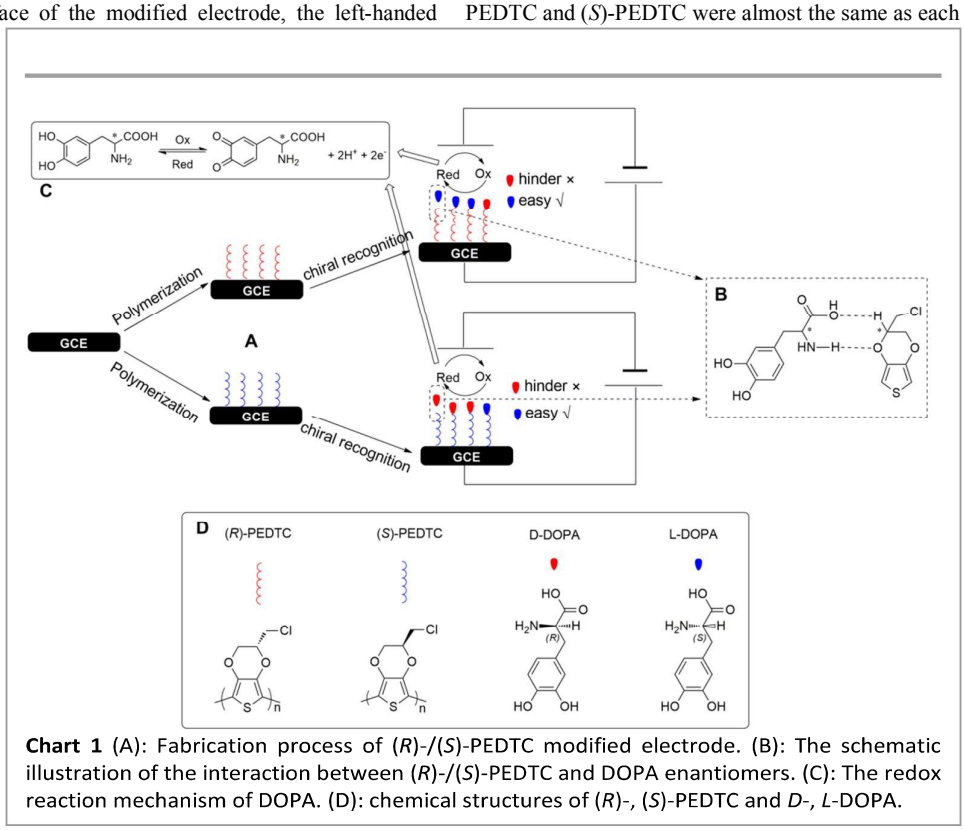


**Chart 1** (A): Fabrication process of (*R*)-/(*S*)-PEDTC modified electrode. (B): The schematic illustration of the interaction between (*R*)-/(*S*)-PEDTC and DOPA enantiomers. (C): The redox reaction mechanism of DOPA. (D): chemical structures of (*R*)-, (*S*)-PEDTC and *D*-, *L*-DOPA.

RSC Advances Accepted Manuscript


This journal is © The Royal Society of Chemistry 20xx

of electrochemical behavior, structural characterization, morphology and thermal stability. However, CD spectra showed a mirror image of (*R*)-PEDTC and (*S*)-PEDTC films in the neutral state. We have shown that, the polymer-modified electrodes are distinctly di□erent for the *D* and *L* enantiomers of DOPA through the electrochemical sensing technologies of SWV and DPV. Thereby, we established the mechanism of chiral recognition as the first examples for chiral PEDOTs electrode materials. However, more intensive studies of this nature are required before a new model of the action of the chiral PEDOT derivatives in promoting enantioselectivity may be proposed.

## Acknowledgements

The authors would like to acknowledge the financial support of this work by the National Natural Science Foundation of China (51263010, 51303073, 51272096), Natural Science Foundation of Jiangxi Province (20142BAB206028) and the Science and Technology Landing Plan of Universities in Jiangxi Province (KJLD14069) and Jiangxi Science and Technology Normal University (YC2014-X27) for their financial support of this work.

## Notes and references

1. L. A. Kane-Maguire and G. G. Wallace, *Chem. Soc. rev.*, 2010, **39**, 2545-2576.
2. R. L. Elsenbaumer, H. Eckhardt, Z. Iqbal, J. Toth and R. H. Baughman, *Mol. Cryst. Liq. Cryst.*, 1985, **118**, 111-116.
3. M. Lemaire, D. Delabouglise, R. Garreau, A. Guy and J. Roncali, *J. Chem. Soc., Chem. Commun.*, 1985, 658-661.
4. M. Salmón and G. Bidan, *J. Electrochem. Soc.*, 1985, **132**, 1897-1899.
5. M. R. Majidi, L. A. P. Kane-maguire and G. G. Wallace, *Polym.*, 1994, **35**, 3113-3115.
6. E. E. Havinga, M. M. Bouman, E. W. Meijer, A. Pomp and M. M. J. Simenon, *Synth. Met.*, 1994, **66**, 93-97.
7. M. R. Majidi, L. A. P. Kane-Maguire and G. G Wallace, *Aust. J. Chem.*, 1998, **51**, 23-30.
8. K. Akagi, G. Piao, S. Kaneko, K. Sakamaki, H. Shirakawa, and M. Kyotani, *Science,* 1998, **282**, 1683-1686.
9. M. Oda, H.-G. Nothofer, G. Lieser, U. Scherf, S. C. J. Meskers and D. Neher, *Adv. Mater.*, 2000, **12**, 362-365.
10. M. Oda, H. G. Nothofer, U. Scherf, V. Šunjić, D. Richter, W. Regenstein and D. Neher, *Macromolecules*, 2002, **35**, 6792-6798.
11. H. Goto and K. Akagi, *Macromolecules*, 2005, **38**, 1091-1098.
12. G. Bidan, S. Guillerez and V. Sorokin, *Adv. Mater.*, 1996, **8**, 157-160.
13. H. Goto, Y. Okamoto and E. Yashima, *Macromolecules*, 2002, **35**, 4590-4601.
14. B. M. W. Langeveld-Voss, R. A. J. Janssen, M. P. T. Christiaans, S. C. J. Meskers, H. P. J. M. Dekkers and E. W. Meijer, *J. Am. Chem. Soc.*, 1996, **118**, 4908-4909.
15. S. Yorozuya, I. Osaka, A. Nakamura, Y. Inoue and K. Akagi, *Synth. Met.*, 2003, **135–136**, 93-94.
16. K. Watanabe, I. Osaka, S. Yorozuya and K. Akagi, *Chem. Mater.*, 2012, **24**, 1011-1024.
17. H. Goto, Y. S. Jeong and K. Akagi, *Macromol. Rapid Commun.*, 2005, **26**, 164-167.
18. Y. Sulaiman and R. Kataky, *Analyst*, 2012, **137**, 2386-2393.
19. P. R. Teasdale and G. G. Walfacet, *Analyst*, 1993, **118**, 329-334.
20. E. M. Sheridan and C. B. Breslin, *Electroanal.*, 2005, **17**, 532-537.
21. K. Shimomura, T. Ikai, S. Kanoh, E. Yashima and K. Maeda, *Nat. Chem.*, 2014, **6**, 429-434.
22. C. Zhang, H. Wang, Q. Geng, T. Yang, L. Liu, R. Sakai, T. Satoh, T. Kakuchi and Y. Okamoto, *Macromolecules*, 2013, **46**, 8406-8415.
23. R. Liu, M. Shiotsuki, T. Masuda and F. Sanda, *Macromolecules*, 2009, **42**, 6115-6122.
24. K. Akagi, S. Guo, T. Mori, M. Goh, G. Piao and M. Kyotani, *J. Am. Chem. Soc.*, 2005, **127**, 14747-14654.
25. S. Y. Oh, K. Akagi and H. Shirakawa, *Macromolecules*, 1993, **26**, 6203-6206.
26. P. Novak, K. Muller, K. S. V. Santhanam and O. Haas, *Chem. Rev.*, 1997, **97**, 207-281.
27. H. Hayasaka, T. Miyashita, K. Tamura and K. Akagi, *Adv. Funct.Mater.*, 2010, **20**, 1243-1250.
28. C. Song, C. Zhang, F. Wang, W. Yang and J. Deng, *Polym. Chem.*, 2013, **4**, 645-652.
29. M. H. El-Newehy, A. S. Elsherbiny and H. Mori, *J. Appl. Polym. Sci.*, 2013, **127**, 4918-4926.
30. L. Groenendaal, F. Jonas, D. Freitag, H. Pielartzik and J. R. Reynolds, *Adv. Mater.*, 2000, **12**, 481-494.
31. H. Goto and K. Akagi, *Macromol. Rapid Commun.*, 2004, **25**, 1482-1486.
32. M. Ding, *Prog. Polym. Sci.*, 2007, **32**, 623-668.
33. Y. S. Jeong and K. Akagi, *J. Mater. Chem.*, 2011, **21**, 10472-10481.
34. H. Goto, *J. Mater. Chem.*, 2009, **19**, 4914-4921.
35. T. Hatano, A. H. Bae, M. Takeuchi, N. Fujita, K. Kaneko, H. Ihara, M. Takafuji and S. Shinkai, *Angew. Chem. Int. Edit.*, 2004, **43**, 465-469.
36. L. Dong, B. Lu, X. Duan, J. Xu, D. Hu, K. Zhang, X. Zhu, H. Sun, S. Ming, Z. Wang and S. Zhen, *J. Polym. Sci. Part A: Polym. Chem.*, 2015, **53**, 2238-2251.
37. D. Hu, L. Zhang, K. Zhang, X. Duan, J. Xu, L. Dong, H. Sun, X. Zhu and S. Zhen, *J. Appl. Polym. Sci.*, 2015, **132**, 41559.
38. D. W. Armstrong, W. Demond and B. P. Czech, *Anal. Chem.*, 1985, **57**, 481-484.
39. L. Zhang, M. Song, Q. Tian and S. Min, *Sep. Purif. Technol.*, 2007, **55**, 388-391.
40. Q. Fu, H. Sanbe, C. Kagawa, K.-K. Kunimoto and J. Haginaka, *Anal. Chem.*, 2003, **75**, 191-198.
41. K. Bodenhofer, A. Hierlemann, J. Seemann, G. Gauglitz, B. Koppenhoefer and W. Gopel, *Nature*, 1997, **387**, 577-580.
42. V. Schurig and W. Buerkle, *J. Am. Chem. Soc.*, 1982, **104**, 7573-7580.
43. V. Schurig, *J. chromatogr. A*, 2001, **906**, 275-299.
44. Z. Chen, T. Nishiyama, K. Uchiyama and T. Hobo, *Anal. Chim. Acta*, 2004, **501**, 17-23.
45. Y. Liu, A. Berthod, C. R. Mitchell, T. L. Xiao, B. Zhang and D. W. Armstrong, *J. chromatogr. A*, 2002, **978**, 185-204.
46. Y. Zhao, W. A. Pritts and S. Zhang, *J. Chromatogr. A*, 2008, **1189**, 245-253.
47. A. Balamurugan, V. Kumar and M. Jayakannan, *Chem. Commun.*, 2014, **50**, 842-845.

RSC Advances Accepted Manuscript

48. H. Ito and S. Shinoda, *Chem. Commun.*, 2015, **51**, 3808-3811.
49. X. Liu and I. P. Hamilton, *J. Am. Chem. Soc.*, 2014, **136**, 17757-17761.
50. R. Kuhn, F. Erni, T. Bereuter and J. Haeusler, *Anal. Chem.*, 1992, **64**, 2815-2820.
51. L. Sánchez-Hernández, M. Guijarro-Diez, M. L. Marina and A. L. Crego, *Electrophoresis*, 2014, **35**, 12-27.
52. N. M. Maier and W. Lindner, *Anal. bioanal. chem.*, 2007, **389**, 377-397.
53. K. C. Ho, W. M. Yeh, T. S. Tung and J. Y. Liao, *Anal. Chim. Acta*, 2005, **542**, 90-96.
54. Y. Huang, Q. Han, Q. Zhang, L. Guo, D. Guo and Y. Fu, *Electrochim. Acta*, 2013, **113**, 564-569.
55. E. Zor, H. Bingol, A. Ramanaviciene, A. Ramanavicius and M. Ersoz, *Analyst*, 2015, **140**, 313-321.
56. Y. J. Kang, J. W. Oh, Y. R. Kim, J. S. Kim and H. Kim, *Chem. Commun.*, 2010, **46**, 5665-5667.
57. Y. Huang, D. Guo, Q. Zhang, L. Guo, Y. Chen and Y. Fu, *RSC Adv.*, 2014, **4**, 33457-33461.
58. S. Pleus and M. Schwientek, *Synth. Met.*, 1998, **95**, 233-238.
59. Y. Yao, L. Zhang, Z. Wang, J. Xu and Y. Wen, *Chin. Chem. Lett.*, 2014, **25**, 505-510.
60. L. Zhang, Y. Wen, Y. Yao, X. Duan, J. Xu and X. Wang, *J. Appl. Polym. Sci.*, 2013, **130**, 2660-2670.
61. L. Zhang, Y. Wen, Y. Yao, Z. Wang, X. Duan and J. Xu, *Chin. Chem. Lett.*, 2014, **25**, 517-522.
62. B. Lu, S. Zhang, L. Qin, S. Chen, S. Zhen and J. Xu, *Electrochim. Acta*, 2013, **106**, 201-208.
63. Z. Wang, J. Xu, B. Lu, S. Zhang, L. Qin, D. Mo and S. Zhen, *Langmuir*, 2014, **30**, 15581-15589.
64. L. Zhang, Y. Wen, Y. Yao, J. Xu, X. Duan and G. Zhang, *Electrochim. Acta*, 2014, **116**, 343-354.
65. Y. Yao, Y. Wen, L. Zhang, Z. Wang, H. Zhang and J. Xu, *Anal. Chim. Acta*, 2014, **831**, 38-49.
66. S. Ming, S. Zhen, K. Lin, L. Zhao, J. Xu and B. Lu, *ACS Appl. Mater. & Inter.*, 2015, **7**, 11089-11098.
67. Q. Peil, G. Zuccarello, M. Ahlskog and O. Inganäs, *Polym.*, 1994, **35**, 1347-1351.
68. B. Lu, J. Yan, J. Xu, S. Zhou and X. Hu, *Macromolecules*, 2010, **43**, 4599-4608.
69. Y. S. Jeong and K. Akagi, *Macromolecules*, 2011, **44**, 2418-2426.
70. G. Inzelt, M. Pineri, J. W. Schultze and M. A. Vorotyntsev, *Electrochim. Acta*, 2000, **45**, 2403-24221.
71. F. Uckert, Y. H. Tak, K. Müllen and H. Bässler, *Adv. Mater.*, 2000, **12**, 905-908.
72. R. Yue, B. Lu, J. Xu, S. Chen and C. Liu, *Polym. J.*, 2011, **43**, 531-539.
73. S. Zhang, J. Hou, R. Zhang, J. Xu, G. Nie and S. Pu, *Eur. Polym. J.*, 2006, **42**, 149-160.
74. Z. Wang, J. Xu, Y. Yao, L. Zhang, Y. Wen, H. Song and D. Zhua, *Sensor Actuat. B-Chem.*, 2014, **196**, 357-369.
75. Q. Han, Q. Chen, Y. Wang, J. Zhou and Y. Fu, *Electroanal.*, 2012, **24**, 332-337.
76. M. Eslami, M. Namazian and H. R. Zare, *Electrochim. Acta*, 2013, **88**, 543-551.
77. R. B. Bazaco, R. Gomez, C. Seoane, P. Bauerle and J. L. Segura, *Tetrahedron Lett.*, 2009, **50**, 4154-4157.
78. L. Chen, F. Chang, L. Meng, M. Li and Z. Zhu, *Analyst*, 2014, **139**, 2243-2248.
79. K. Chun, T. H. Kim, O. S. Lee, K. Hirose, T. D. Chung, D. S. Chung and H. Kim, *Anal. Chem.*, 2006, **78**, 7597-7600.

RSC Advances Accepted Manuscript



This journal is © The Royal Society of Chemistry 20xx

**GRAPHICAL ABSTRACT**

This manuscript reports a couple of novel polymers of side-chain functionalized PEDOT, *i.e.*, poly((R)-2-(chloromethyl)-2,3-dihydrothieno[3,4-b][1,4]dioxine) ((R)-PEDTC) and poly((S)-2-(chloromethyl)-2,3-dihydrothieno[3,4-b][1,4]dioxine) ((S)-PEDTC). The new polymers as chiral electrodes can be employed to successfully recognize 3,4-dihydroxyphenylalanine (DOPA) enantiomers and we also discussed the mechanism of chiral recognition.

Graphical Abstract Figure

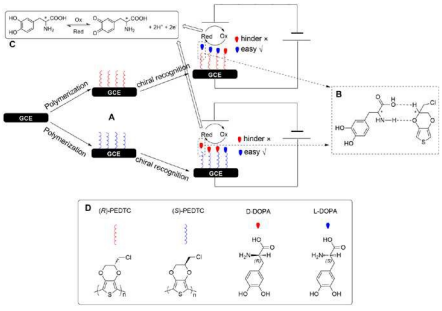


RSC Advances Accepted Manuscript